Floating under a levitating liquid

Benjamin Apffel, Filip Novkoski, Antonin Eddi, Emmanuel Fort

Floating under a levitating liquid

Benjamin Apffel[1,†], Filip Novkoski[1,†], Antonin Eddi[2], Emmanuel Fort[1,*]

[1]ESPCI Paris, PSL University, CNRS, Institut Langevin, 1 rue Jussieu, F-75005 Paris, France.

[2] PMMH, CNRS, ESPCI Paris, Université PSL, Sorbonne Université, Université de Paris, F-75005, Paris, France

*Correspondence to: emmanuel.fort@espci.fr

†The authors contributed equally

Abstract

When placed upside down, a liquid surface is known to fall if it is above a certain size. Gravity acting on the lower liquid interface has a destabilizing effect called Rayleigh-Taylor instability[1,2]. Among the many methods that have been developed to prevent the liquid from falling[3–6], vertical shaking has proved efficient and been studied in detail[7–13]. Stabilization is the result of the dynamical averaging effect of the oscillating effective gravity. Vibrations of liquids also induce other paradoxical phenomena such as the sinking of air bubbles [14–19] or stabilization of the liquid layer above sinking objects[20]. Here, we show that the dynamic stabilization creates a stable buoyancy on the lower interface as if gravity were inverted. Bodies can thus float upside down on the lower interface of levitating liquid layers. We take advantage of the excitation resonance of the supporting air layer to perform experiments with large levitating liquid volumes up to half a liter and a width up to 20 cm. The experimental findings are explained by the dynamical stabilization of the buoyant equilibrium which exists on the lower interface. This model also predicts a minimal excitation needed to withstand falling which is dependent on the floater mass. Experimental observations confirm the possibility of selective falling of heavy bodies. Our findings invite us to rethink all interfacial phenomena in this exotic and counter-intuitive stable configuration.

Maintaining a liquid upside-down is challenging but various situations in which the liquid can be sustained are known. In the case of a limited surface size, capillary forces have a stabilizing effect [21–23]. Alternatively, for large but thin liquid layers suspended under a plate, capillarity opposes gravity [24,25]. In the latter case, the liquid interface does not stay flat but is destabilized in a regular

pattern of hanging droplets. This instability driven by gravity, known as the Rayleigh-Taylor instability, occurs at the interface between two fluids whenever a denser one is placed over a lighter one[1,2]. Several approaches have been used to stabilize the liquid layer such as temperature gradients [3], electric [4] or magnetic fields [5], rotational motion [6] and vertical vibrations [7–13]. In the latter case, the amplitude of the vibration needs to be increased with the surface size. The maximum amplitude is set by the triggering of another instability called the Faraday instability which tends to destabilize fluid surfaces above a certain acceleration threshold [26,27]. However, this threshold can be raised by increasing the fluid viscosity [28]. Hence, the upside-down liquid volume can be large provided the viscosity is properly chosen.

The vertical vibration of a fluid also induces air bubbles to sink below a certain depth in the liquid defying the well-known Archimedes' principle [14–20]. This effect has been studied for industrial applications in gas holdup and mixing in bubble column reactors [29].

Here, we investigate the effect of the vertical vibrations on the buoyancy of bodies immersed in levitating liquid layers and in particular at their lower interface. Our experimental setup consists of a Plexiglas container fixed on a shaker vibrated vertically at frequency $\omega/2\pi$ with an amplitude A (Fig. 1a). The container is filled with silicon oil or glycerol with high viscosity (typically ranging from 0.2 Pa.s to 1 Pa.s) to increase the Faraday instability threshold [8]. Though they have different physical properties, both liquids exhibit similar behavior provided that their viscosity is large enough. In particular, the wetting conditions appear to have limited influence thanks to dynamical effects on the contact line. Air bubbles are observed to sink when placed below a critical depth. This behavior which defies standard buoyancy can be explained by a simple model taking into account the kinetic force, also called the Bjerknes force [30], exerted on the bubble in the oscillating bath [14,16] (see Supplementary Materials and Movie 1 for details). By expanding an already sunken bubble, we create an air layer trapped below a levitated liquid layer (Fig. 1b and Supplementary Movie 2). Its lower interface is stabilized by the vertical shaking, preventing the release of the trapped air. This air layer is acting as a vertical spring loaded with the liquid mass placed upon it and driven by the shaker (Fig. 1c). It can be modeled by a driven damped harmonic oscillator $\ddot{z} + 2\Gamma\omega_{\mathrm{res}}\dot{z} + \omega_{\mathrm{res}}^2 z = A\omega^2\cos(\omega t)$ with ω_{res} the resonance frequency of the air layer and Γ the damping ratio due to the shearing induced by the relative motion between the levitating liquid layer and the bath walls (see Supplementary Information). In the laboratory frame, the normalized

oscillation amplitude $A_l(\omega)/A$ and its associated relative phase $\phi_l(\omega)$-ϕ compared to the shaker clearly show the expected resonance behavior (Fig 1c and 1d). The air layer thus enables the enhancement of the excitation amplitude of the shaker by more than one order of magnitude. Near resonance, the amplitude is high enough to excite the Faraday instability on both sides of the fluid layer (see inset Fig. 1d and Supplementary Movie 3). This resulting "rain" emitted from the lower interface induces a thinning of the fluid layer which can be avoided by simply reducing the excitation amplitude. Provided the spring-mass oscillation is properly tuned, there is no restriction in the number of sustained levitating layers which can be piled on top of one another (see Fig. 2e and Supplementary Movie 4).

As mentioned before, the vertical vibrations have a stabilizing effect on the lower fluid interface. This can be interpreted as a Kapitza effect which consists of a dynamical stabilization of an inverted pendulum by vertical shaking [31,32]. Solving the Bernoulli equation for the fluid shows that the interface height $\zeta(k)$ at the spatial wavenumber k behaves like an inverted pendulum. The spatial mode satisfies $\ddot{\zeta} + \left[\omega_0(k)^2 + \frac{A_l^2 k^2}{2}\omega^2\right]\zeta = 0$ with $\omega_0(k)^2 = -gk + (\gamma k^3)/\rho_l$ the gravito-capillary dispersion relation with inverted gravity. Without vibrations, the oscillator is unstable for small enough k ($\omega_0(k)^2<0$) leading to the Rayleigh-Taylor instability while large wave numbers are stabilized by capillarity. The last term in the equation arises from the modulation of the effective gravity. In gravitational regime, the stabilization is reached for wavenumbers satisfying $k > 2g/A_l^2\omega^2$ (see Supplementary Information). The limited size L for the bath sets a maximum limit to the observed excitable wavenumber $k>2\pi/L$ (only anti-symmetric modes satisfying volume conservation are considered). As a consequence, the stability of the interface is obtained for oscillating liquid velocities $v_l = A_l\omega$ above a critical velocity $v_l^* = \sqrt{gL/\pi} < v_l$. There seems to be no size limit for stabilization. The maximum levitated mass was 0.5 L in a 12x12 cm^2 container, and the max length achieved was 20 cm. The limitations in mass are only due to the shaker. In addition, no decay in time was observed and the layers remained stable for arbitrary long times. Figure 1f shows the oscillating velocity v_l^* needed to stabilize baths with lengths L up to 18 cm (insets show views of levitating layers for L=2 cm and L=18 cm, see Supplementary Movie 5). Other effects might have an influence on the stability, such as friction or the flows formed at the boundary, but their influence is limited (see Supplementary Information).

We now focus on objects floating at the inverted interface of the levitating fluid layer. Archimedes' principle states that the upward buoyant force exerted on an immersed body, whether fully or partially submerged, is equal to the weight of the displaced fluid. Although this may seem counterintuitive, the transpose symmetric position at the lower interface (see Fig 2a) also exhibits an upward buoyant force equal to the weight of displaced liquid. Figure 2b shows the typical potential exerted on a floating body without taking into account the dynamic effects (see Supplementary information for details). The two equilibrium positions associated with each interface are clearly visible. However, while the upper position is stable, the lower is not: pushing the body down/up would make it fall/float to the upper interface. Taking into account the dynamical effect, i.e. the time averaged effect of the oscillations, provides an additional stabilizing dynamical potential around the two equilibrium positions (see inset Fig. 2b). Averaged small displacements Z_b of the floater around the two equilibrium positions satisfies the same dynamical equation $\ddot{Z}_b + \omega_b^2(1+\alpha)Z_b = 0$, ω_b being the angular frequency associated with the buoyancy force and $\alpha = \frac{\omega_b^2}{2}\left(\frac{A_l\omega}{g}\right)^2$ the correction induced by the averaged dynamical effects (see Supplementary Information for details). While, the dynamical effects increase the stability of the equilibrium at the upper interface $\left(\omega_b^2 > 0, \alpha > 0\right)$, the unstable static equilibrium at the lower interface ($\omega_b^2 < 0$) is stabilized by the dynamical effects (α<0). It is interesting to note that similar dynamical stabilizations were observed with a washer mounted on a vibrated inverted pendulum[20]. The floater stability is reached for liquid velocity v_l above a critical value given by $v_b^* = \sqrt{2g/|\omega_b|} < v_l$. It is thus possible to have floating bodies with varying density above and below the levitating liquid layers (see Figure 2c). Hence the vibration not only gives stability of the lower horizontal interface of a liquid but also permits a vertical stabilization of the unstable equilibrium position that a floater would experience on such interface. This dynamical "anti-gravity" enables boats to float on both interfaces (Fig. 1e, see Supplementary Movie 6).[33] Note that the drag force induced by secondary flows due to recirculation in the liquid layer should not significantly change the vertical equilibrium position (see Supplementary Movie 2 and Supplementary Information).

The previous stability conditions suggest that the critical fluid velocity to stabilize a floater v_b^* and the liquid layer v_l^* are different and that sufficiently massive floaters should fall before the layer collapses ($v_b^* > v_l^*$). We performed the experiments in silicon oil with spherical floaters of

increasing mass, the heaviest one being almost neutrally buoyant (Figure 3). Contrary to light floaters which fall with the liquid layer as the excitation amplitude is decreased, heavier floaters fall before the levitating layer gets destabilized (see inset Figure 3 and Supplementary Movie 7). The theoretical critical velocity v_b can be exactly computed for spheres without any adjustable parameters (solid blue line). The expected range of masses for which $v_\mathrm{b}^* > v_\mathrm{l}^*$ is consistent with the experimental findings (blue area in Fig. 3) and the values v_b^* are in reasonable agreement. Discrepancy occurs for almost neutrally buoyant floaters (as also for buoyant equilibrium position). In this limit, new phenomena are observed such as a small relative motion of floaters with respect to the surrounding fluid layer which seems to play a significant role in the floater equilibrium.

This counter-intuitive upside-down buoyancy phenomenon suggests that the stabilization of Rayleigh-Taylor instability through vibrations can be considered not only in itself but also as a playground for new experiments in unexplored conditions. Under this perspective, many phenomena that occur at the interface between air and liquids could be investigated and reformulated in this new exotic configuration such as transport and segregation.

References

1. Lord Rayleigh. Investigation of the character of the equilibrium of an incompressible heavy fluid of variable density. *Proceedings of the London mathematical society* **14**, 170–177 (1883).
2. Lewis, D. J. & Taylor, G. I. The instability of liquid surfaces when accelerated in a direction perpendicular to their planes. II. *Proceedings of the Royal Society of London. Series A. Mathematical and Physical Sciences* **202**, 81–96 (1950).
3. Burgess, J. M., Juel, A., McCormick, W. D., Swift, J. B. & Swinney, H. L. Suppression of Dripping from a Ceiling. *Phys. Rev. Lett.* **86**, 1203–1206 (2001).

4. Petropoulos, R., Papageorgiou, D. T. & Petropoulos, P. G. On the control and suppression of the Rayleigh-Taylor instability using electric fields. *Physics of Fluids* **26**, 022115 (2014).
5. Rannacher, D. & Engel, A. Suppressing the Rayleigh-Taylor instability with a rotating magnetic field. *Phys. Rev. E* **75**, 016311 (2007).
6. Tao, J. J., He, X. T., Ye, W. H. & Busse, F. H. Nonlinear Rayleigh-Taylor instability of rotating inviscid fluids. *Phys. Rev. E* **87**, 013001 (2013).
7. Wolf, G. H. The dynamic stabilization of the Rayleigh-Taylor instability and the corresponding dynamic equilibrium. *Z. Physik* **227**, 291–300 (1969).
8. Wolf, G. H. Dynamic Stabilization of the Interchange Instability of a Liquid-Gas Interface. *Phys. Rev. Lett.* **24**, 444–446 (1970).
9. Lapuerta, V., Mancebo, F. J. & Vega, J. M. Control of Rayleigh-Taylor instability by vertical vibration in large aspect ratio containers. *Phys. Rev. E* **64**, 016318 (2001).
10. Kumar, S. Mechanism for the Faraday instability in viscous liquids. *Phys. Rev. E* **62**, 1416–1419 (2000).
11. Pototsky, A. & Bestehorn, M. Faraday instability of a two-layer liquid film with a free upper surface. *Phys. Rev. Fluids* **1**, 023901 (2016).
12. Pototsky, A., Oron, A. & Bestehorn, M. Vibration-induced floatation of a heavy liquid drop on a lighter liquid film. *Physics of Fluids* **31**, 087101 (2019).
13. Sterman-Cohen, E., Bestehorn, M. & Oron, A. Rayleigh-Taylor instability in thin liquid films subjected to harmonic vibration. *Physics of Fluids* **29**, 052105 (2017).
14. Baird, M. H. I. Resonant bubbles in a vertically vibrating liquid column. *The Canadian Journal of Chemical Engineering* **41**, 52–55 (1963).

15. Jameson, G. J. The motion of a bubble in a vertically oscillating viscous liquid. *Chemical Engineering Science* **21**, 35–48 (1966).

16. Sorokin, V. S., Blekhman, I. I. & Vasilkov, V. B. Motion of a gas bubble in fluid under vibration. *Nonlinear Dyn* **67**, 147–158 (2012).

17. Blekhman, I. I., Blekhman, L. I., Vaisberg, L. A., Vasil'kov, V. B. & Yakimova, K. S. "Anomalous" phenomena in fluid under the action of vibration. *Dokl. Phys.* **53**, 520–524 (2008).

18. Blekhman, I. I., Blekhman, L. I., Sorokin, V. S., Vasilkov, V. B. & Yakimova, K. S. Surface and volumetric effects in a fluid subjected to high-frequency vibration. *Proceedings of the Institution of Mechanical Engineers, Part C: Journal of Mechanical Engineering Science* **226**, 2028–2043 (2012).

19. Zen'kovskaja, S. M. & Novosjadlyj, V. A. Influence of vertical oscillations on bilaminar system with a non-rigid interface , vol. 48, no. 9, pp 1710-1720. *Zhurnal vychislitel'noj matematiki i matematicheskoj fiziki* **48**, 1710–1720 (2008).

20. Chelomei, V. N. Mechanical paradoxes caused by vibrations. *Soviet Physics Doklady* **28**, 387 (1983).

21. Young, T. III. An essay on the cohesion of fluids. *Philosophical Transactions of the Royal Society of London* **95**, 65–87 (1805).

22. Thomson, W. LX. On the equilibrium of vapour at a curved surface of liquid. *The London, Edinburgh, and Dublin Philosophical Magazine and Journal of Science* **42**, 448–452 (1871).

23. Gennes, P.-G. de, Brochard-Wyart, F. & Quere, D. *Capillarity and Wetting Phenomena: Drops, Bubbles, Pearls, Waves*. (Springer Science & Business Media, 2013).

24. Fermigier, M., Limat, L., Wesfreid, J. E., Boudinet, P. & Quilliet, C. Two-dimensional patterns in Rayleigh-Taylor instability of a thin layer. *Journal of Fluid Mechanics* **236**, 349–383 (1992).

25. Myshkis, A. D., Babskii, V. G., Kopachevskii, N. D., Slobozhanin, L. A. & Tyuptsov, A. *Low-Gravity Fluid Mechanics. Mathematical Theory of Capillary Phenomena.* (Springer-Verlag, 1987).

26. Faraday, M. On a Peculiar Class of Acoustical Figures; and on Certain Forms Assumed by Groups of Particles upon Vibrating Elastic Surfaces. *Philosophical Transactions of the Royal Society of London* **121**, 299–340 (1831).

27. Douady, S. Experimental study of the Faraday instability. *J. Fluid Mech.* **221**, 383–409 (1990).

28. Kumar, K. & Tuckerman, L. S. Parametric instability of the interface between two fluids. *J. Fluid Mech.* **279**, 49–68 (1994).

29. Elbing, B. R., Still, A. L. & Ghajar, A. J. Review of Bubble Column Reactors with Vibration. *Ind. Eng. Chem. Res.* **55**, 385–403 (2016).

30. Bjerknes, V. F. K. *Fields of Force: Supplementary Lectures, Applications to Meteorology*. (Columbia University Press/The Macmillan Company, 1906).

31. Kapitza, P. L. Dynamic stability of a pendulum when its point of suspension vibrates. *Soviet. Phys. JETP* **21**, 588–597 (1951).

32. Krieger, M. S. Interfacial fluid instabilities and Kapitsa pendula. *Eur Phys J E Soft Matter* **40**, 67 (2017).

33. Landau, L. D. & Lifshitz, E. M. *Mechanics*. (Pergamon Press, 1969).

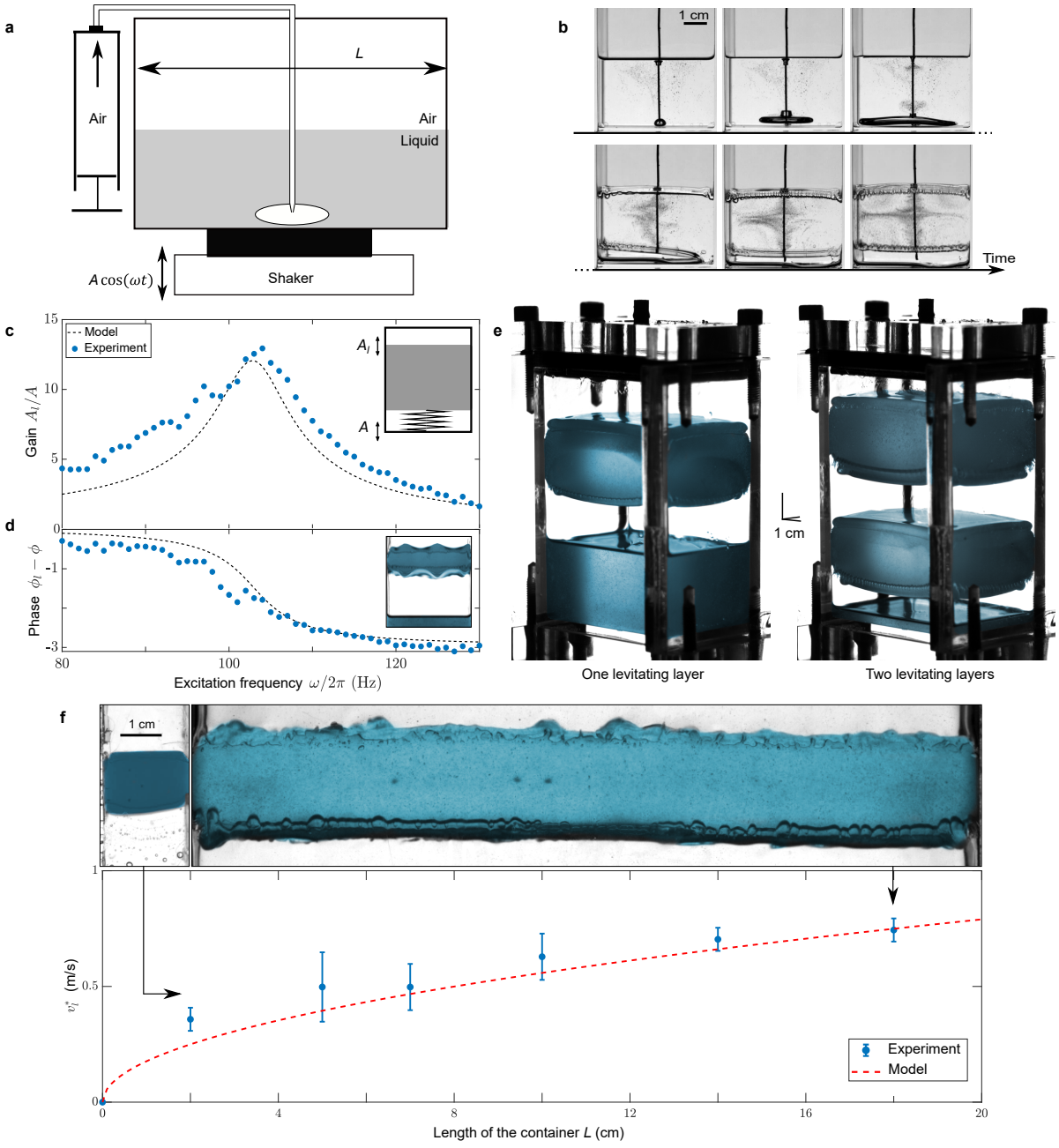

Figure 1 Levitating liquid layer stabilized by Kapitza effect. a, Experimental setup composed of a Plexiglas container of various sizes (up to 20 cm in width) attached on a vertically oscillating shaker with amplitude A and frequency $\omega/2\pi$. The liquid is either glycerol or silicon oil with high viscosity (typically 0.5 Pa.s). The bubbles are created by injecting air with a syringe through a long needle. We operate at room temperature (20°C). **b**, Image sequence of the creation of the air layer obtained by injecting air at the bottom of the oscillating liquid bath

through a needle. The sinking bubble grows until it completely fills the bottom of the bath (see Supplementary Movie 1 and 2). **c**, Increase of the liquid layer vertical amplitude A_l/A and **d**, relative phase shift ϕ_l-ϕ of the liquid oscillations compared with that of the shaker as a function of the excitation frequency $\omega/2\pi$. Insets: Schematics of the spring-mass systems composed of the air layer loaded with the levitating liquid and image of Faraday instability triggered on the two opposite surfaces of the levitating liquid layer of silicon oil (see Supplement Movie 3). The experimental data (full circles) are fitted with the mass-spring model with fitting parameters $\omega/2\pi$ = 103 Hz and Γ = 0.04 (dashed line, see Supplementary Information for details). **e**, Digitally colorized three-quarter views of the oscillating containers with one and two levitating liquid layers of silicon oil (see Supplementary Movie 4). **f**, Threshold excitation velocity $A_l\omega$ for Kapitza stabilization of the liquid layer as a function of the length L of the container: experimental data (circles, error bars correspond to extremal values over 5 experiments) and model $v_l^* = \sqrt{gL/\pi}$ (dashed line). Side views of the levitating bath in a 2 cm and 18 cm wide container are presented below (see Supplementary Movie 5).

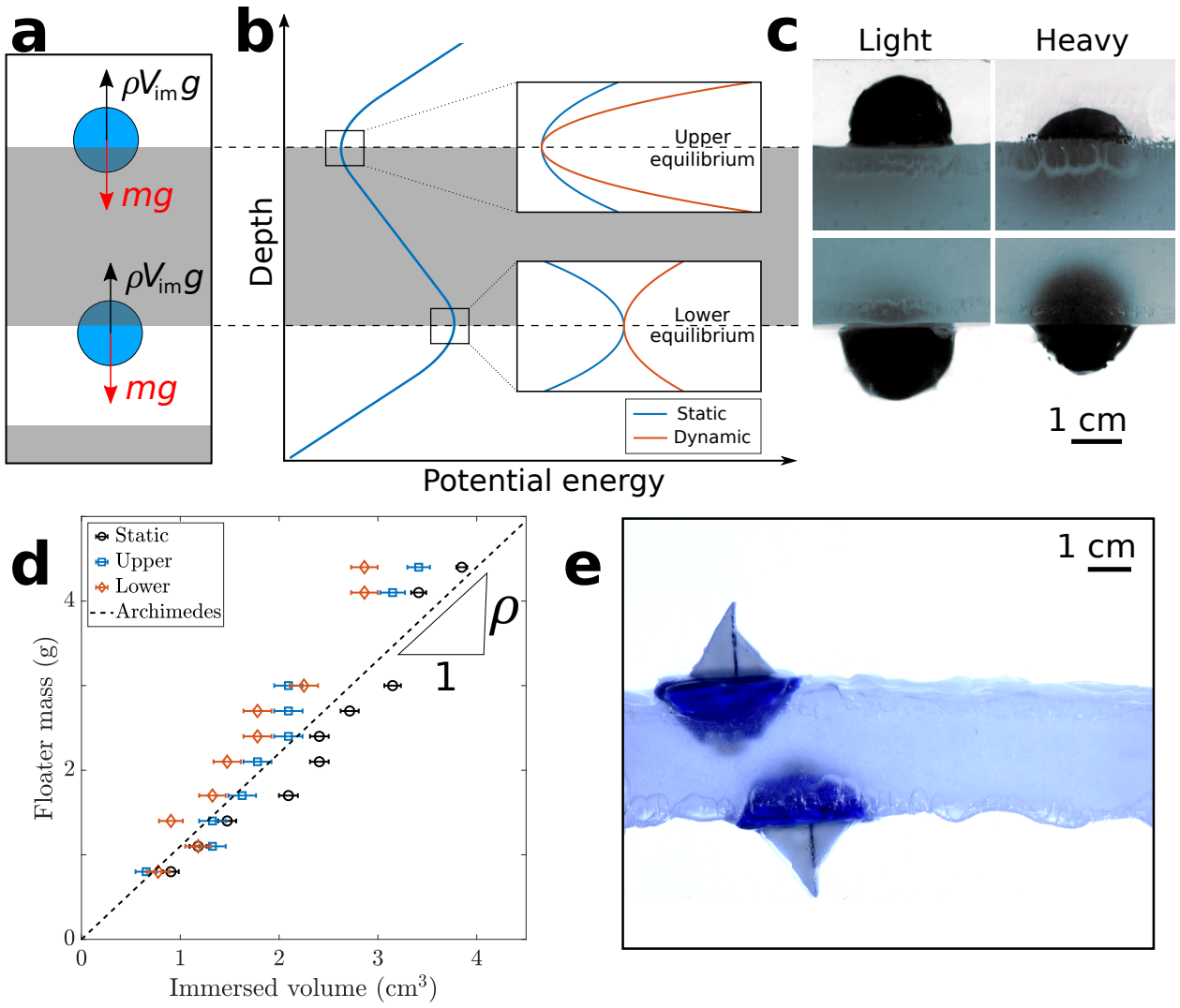

Figure 2 Archimedes' principle over and under a levitating liquid layer. a, Schematics of the force balance at the two opposing interfaces with the buoyant force cancelling the weight of immersed bodies. **b**, Typical profile of the static potential along the vertical direction z neglecting the dynamical effects. Two equilibrium positions appear at each interface, the lower one being unstable. Insets: close up of the potential near the equilibrium positions with the addition of the dynamical stabilizing effect (red line, see Supplementary Information). **c**, Side views of 2 cm diameter plastic spheres floating upwards and downwards with lower (left) and higher density (right). **d**, Time averaged equilibrium positions for 2 cm diameter spheres with varying mass as a function of the immersed volume at the upper (squares) and lower interface

(diamonds). Circles are equilibrium positions obtained without shaking. The dashed line is given by the Archimedes' principle with experimentally measured ρ_l=1.1 kg/L for glycerol. The error bars correspond to extremal values over 5 measurements. **e**, Boats floating above and below over and under a levitated liquid layer (see Supplementary Movie 6).

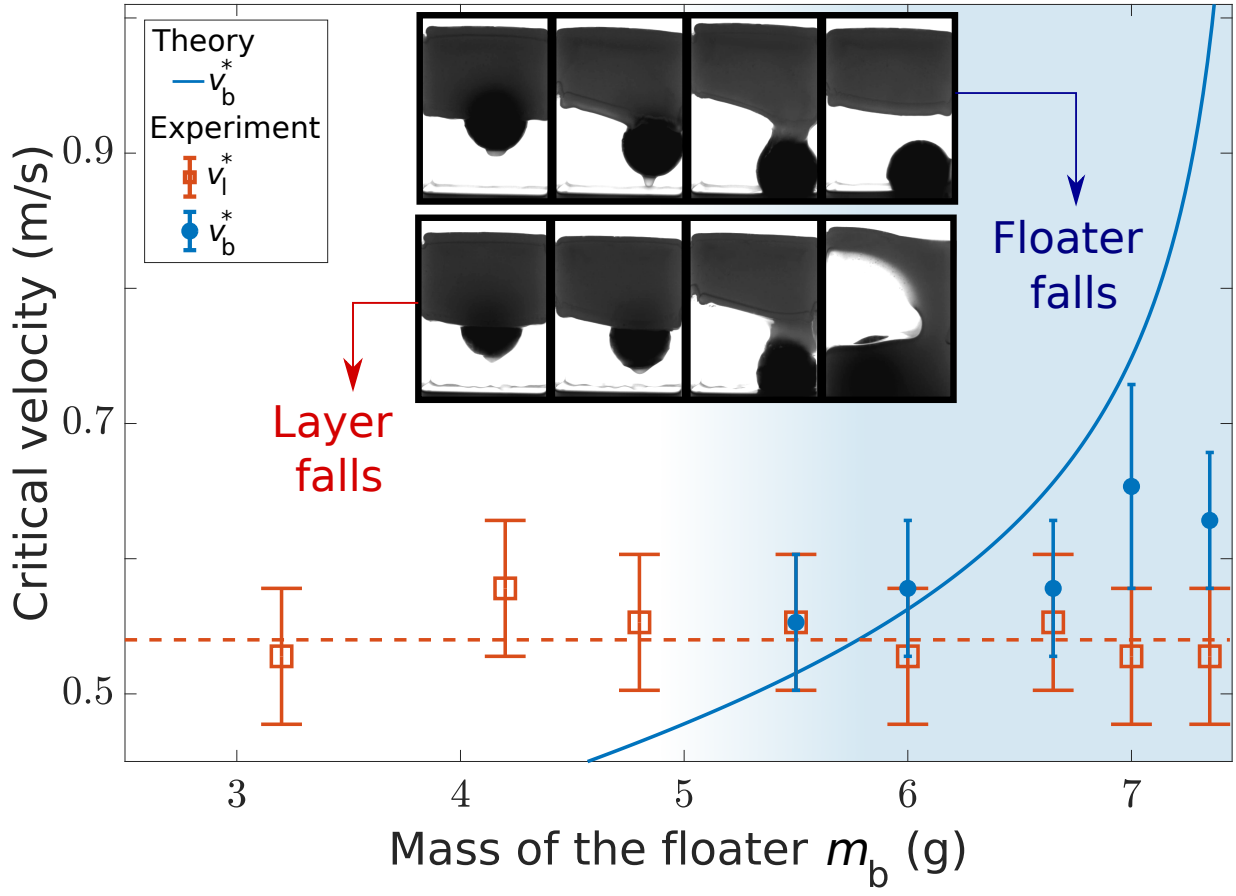

Figure 3 Floater and liquid layer stability. Critical velocities for the stability of the liquid layer v_l^* and for the floater v_b^* as a function of the floater mass m_b. The experiments are performed in a 4x5 cm^2 container with silicon oil and a spherical floater of 2.5 cm with various masses. The model (blue line) based on dynamic stabilization uses the liquid density measured experimentally ρ=0.92 kg/L and no adjustable parameter. Above a certain floater mass $v_b^* > v_l^*$ (blue area) the floater can fall while the liquid layer remains stable. The error bars correspond to extremal values over 3 measurements. The dashed red line is the mean value of the v_l^* measurements. Inset image sequences of the experiment showing the layer falling at v_l^* for $m_{fl} = 4.8$ g and showing the floater falling at v_b^* for $m_b = 6.6$ g (see Supplementary Movie 7).

Acknowledgments: The authors are grateful to Suzie Protière, Arnaud Lazarus, Sander Wildeman and the colleagues and students of "Projets Scientifiques en Equipes" for insightful discussions. The authors thank the support of AXA research fund and the French National Research Agency LABEX WIFI (ANR-10-LABX-24).

Author contributions: All the authors discussed, interpreted the results and conceived the theoretical framework. E. F. gave the initial idea. B. A. and F. N. designed and performed the experiments. B. A., F. N. and E. F. wrote the paper. All authors reviewed the manuscript.

Competing interests: Authors declare no competing interests.

Additional information: Supplementary Information and Movies are available for this paper. Correspondence and requests for materials should be addressed to E. F.

Data availability: All the datasets generated during the current study are available in the Supplementary Information.